Supplementary Information

Selective Catalytic NO_x Reduction by H_2 in Excess O_2 over Pt/Zirconium Phosphate Nanosheet.

Keisuke Awaya,*[a] Yuka Sato,[b] Aoi Miyazaki,[b] Mana Furukubo,[b] Koshi Nishiyama,[b] Masayuki Tsushida,[c] Shintaro Ida,[d] Junya Ohyama,[a,d] Masato Machida*[a,d]

a) Faculty of Advanced Science and Technology, Kumamoto University; 2-39-1, Kurokami, Chuo-ku, Kumamoto, 860-8555, Japan.

b) Graduate School of Science and Technology, Kumamoto University; 2-39-1, Kurokami, Chuo-ku, Kumamoto, 860-8555, Japan.

c) Technical Division, Kumamoto University; 2-39-1, Kurokami, Chuo-ku, Kumamoto, 860-8555, Japan.

d) Institute of Industrial Nanomaterials (IINa), Kumamoto University; 2-39-1, Kurokami, Chuo-ku, Kumamoto, 860-8555, Japan.

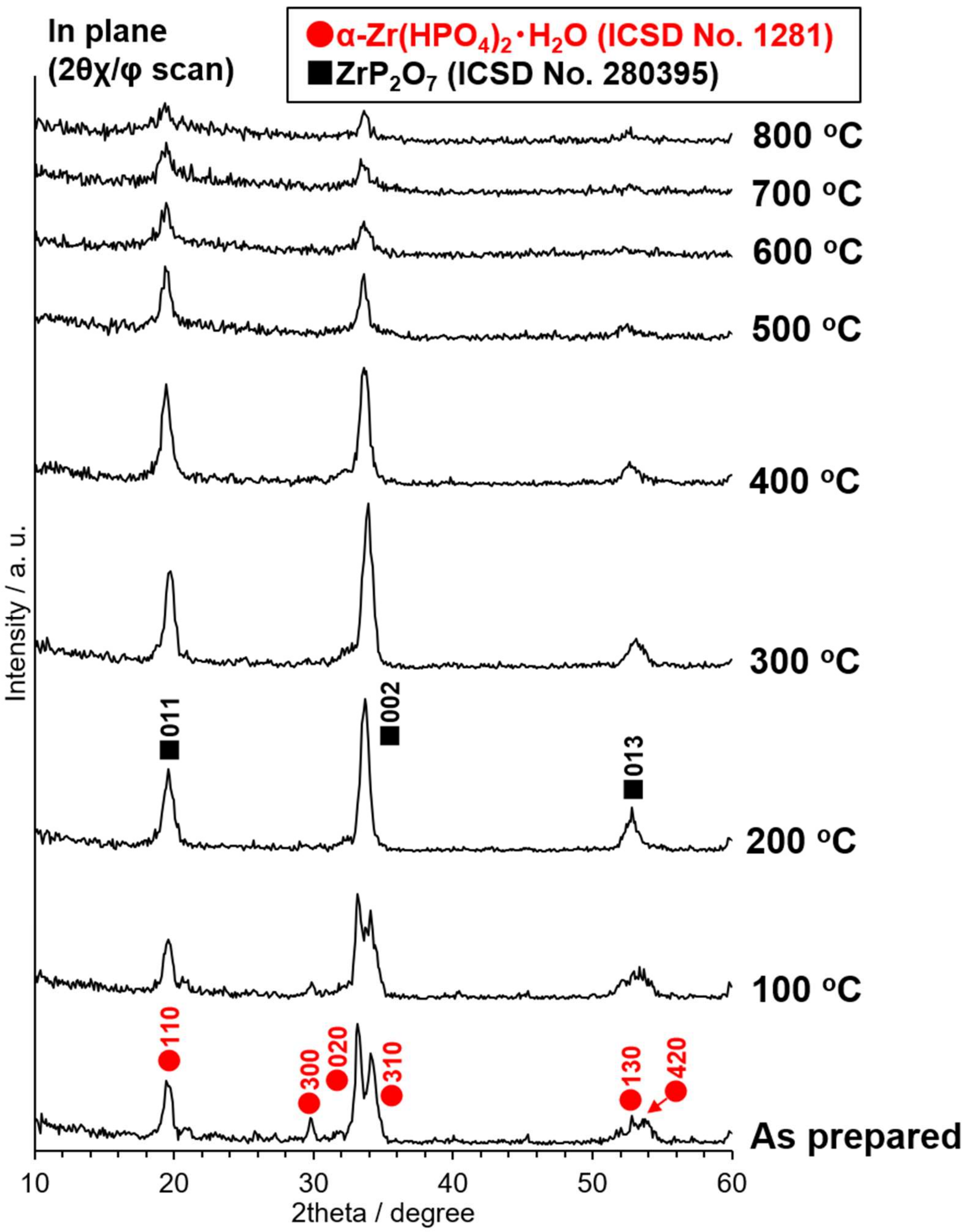

Figure S1. In-plane XRD patterns (2θχ/φ scan) of the ZrP nanosheet spin-coating film deposited on a Si wafer before and after annealing at 100-800 ℃ for 1 h.

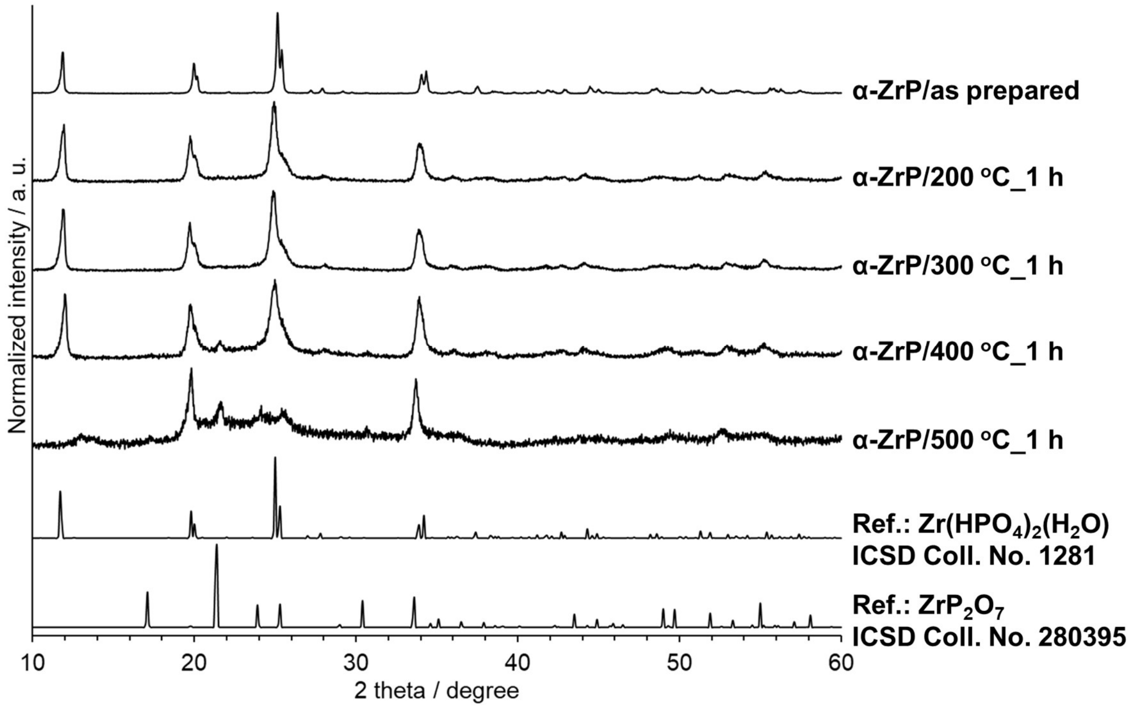

Figure S2. Powder XRD patterns (2θ/θ scan) of the α-ZrP (α-$Zr(HPO_4)_2 \cdot H_2O$) before and after annealing at 200-500 ℃ for 1 h, ICSD #1281 (α-$Zr(HPO_4)_2 \cdot H_2O$), and ICSD #280395 (ZrP_2O_7).

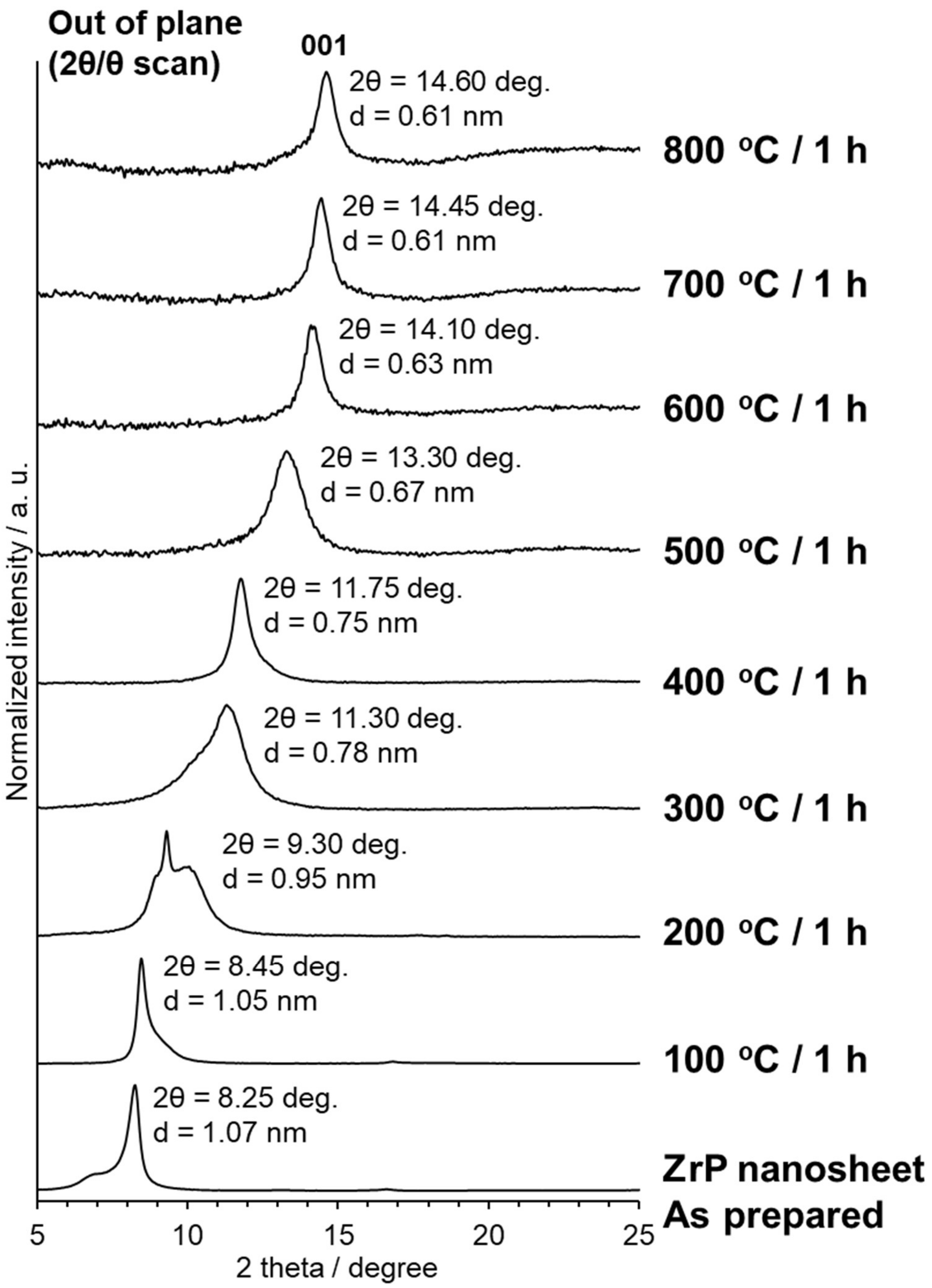

Figure S3. Out-of-plane XRD patterns (2θ/θ scan) of the ZrP nanosheet spin-coating film deposited on a Si wafer before and after annealing at 100-800 ℃ for 1 h.

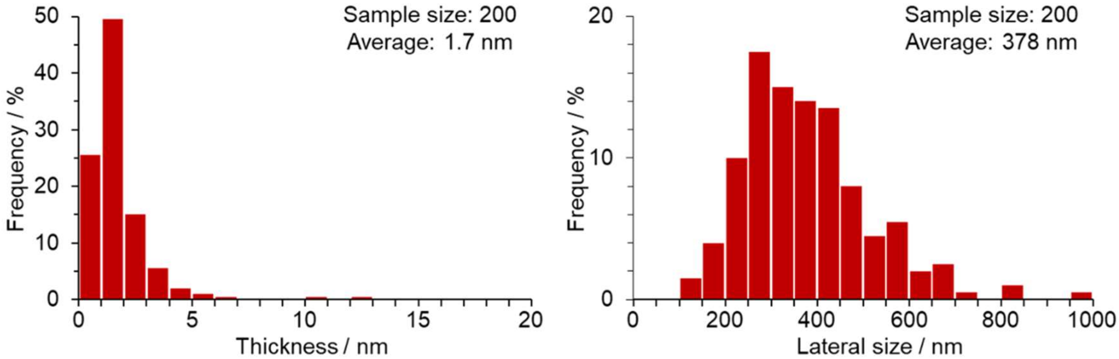

Figure S4. Thickness and lateral size distributions of the ZrP nanosheet deposited on a Si wafer (analysis of AFM images).

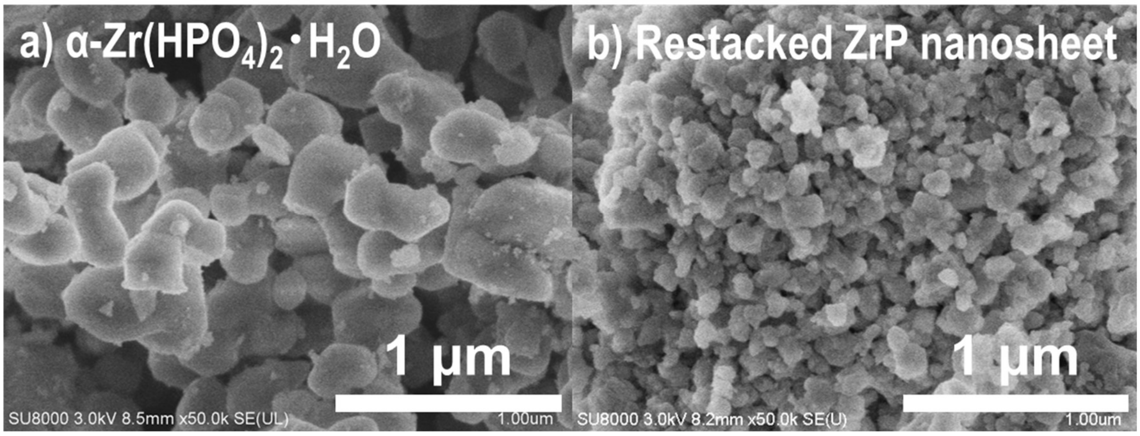

Figure S5. FE-SEM images of the (a) α-ZrP (α-$Zr(HPO_4)_2 \cdot H_2O$) and (b) restacked ZrP nanosheet.

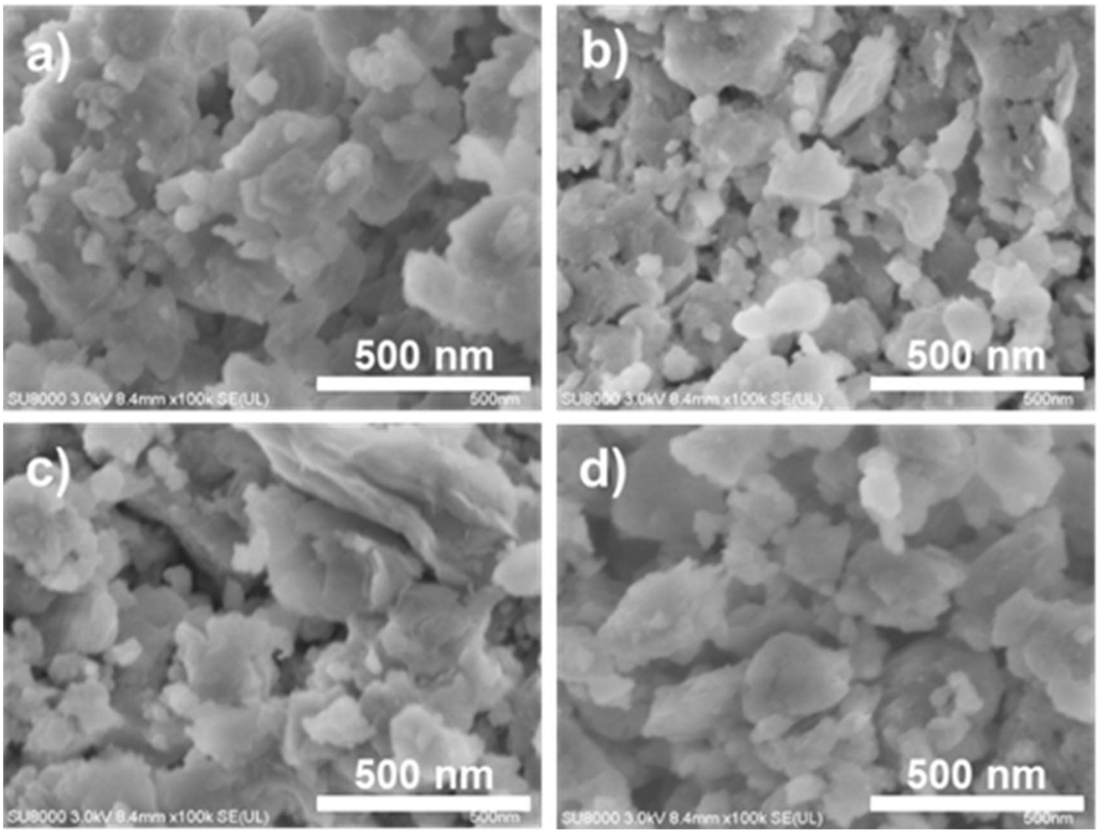

Figure S6. FE-SEM images of (a) 0.08, (b) 0.14, (c) 0.22, and (d) 0.49 wt% Pt (ads.)/ZrP nanosheet.

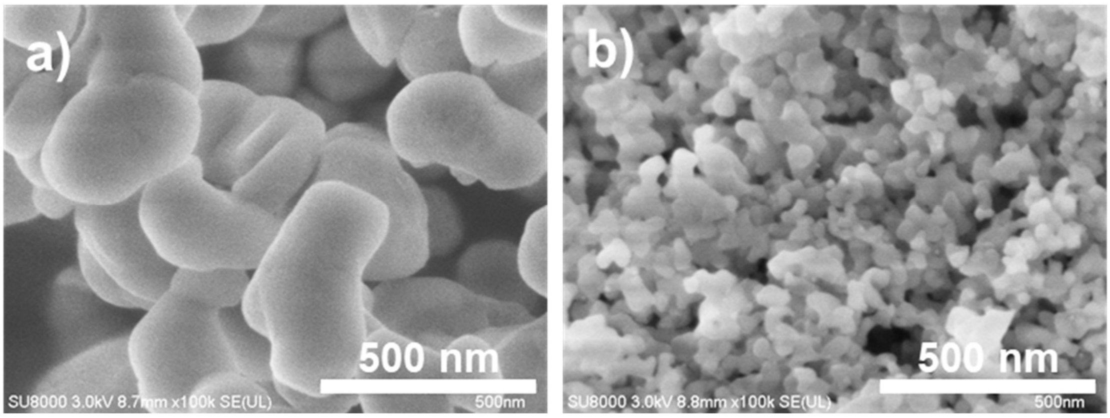

Figure S7. FE-SEM images of the (a) 0.5 wt% Pt (ads.)/α-$Zr(HPO_4)_2 \cdot H_2O$ and (b) 0.4 wt% Pt (ads.)/ZrP_2O_7.

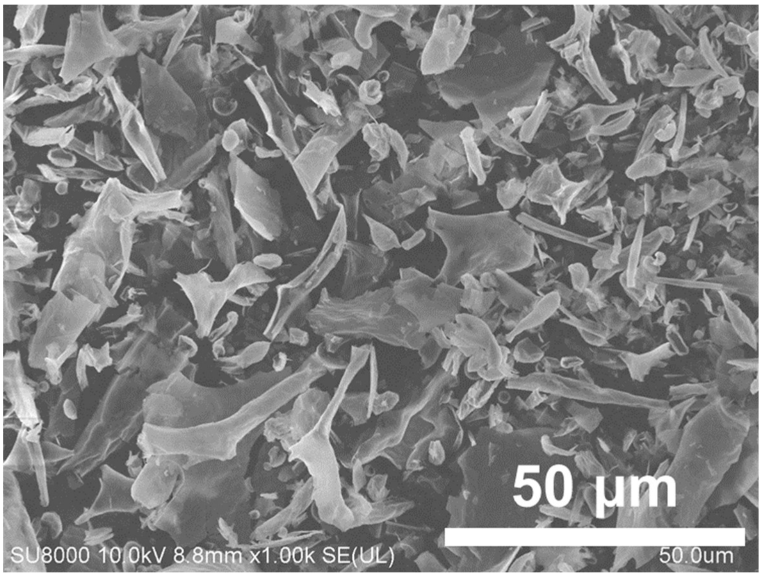

Figure S8. FE-SEM image of the freeze-dried ZrP nanosheet.

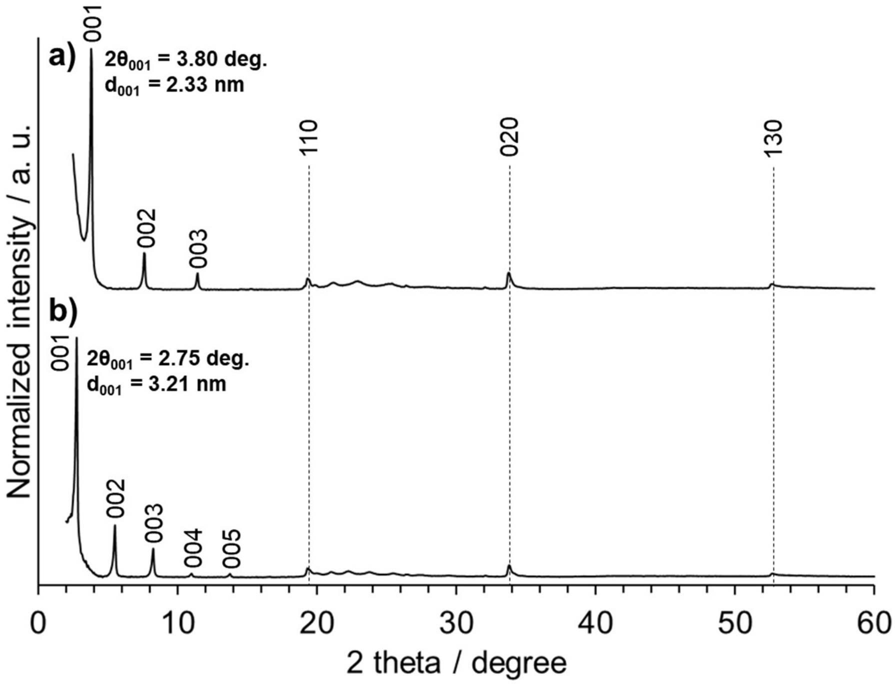

Figure S9. Powder XRD patterns (2θ/θ scan) of the (a) hexylamine (HA)- and the (b) decylamine (DA)-restacked ZrP nanosheet.

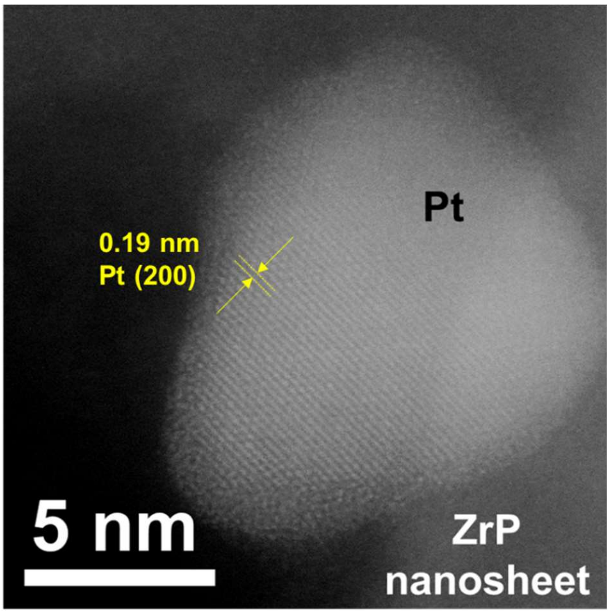

Figure S10. A HAADF-STEM image of the Pt (particle size ~ 14 nm) particle on ZrP nanosheet (0.49 wt% Pt (ads.)/ZrP nanosheet).

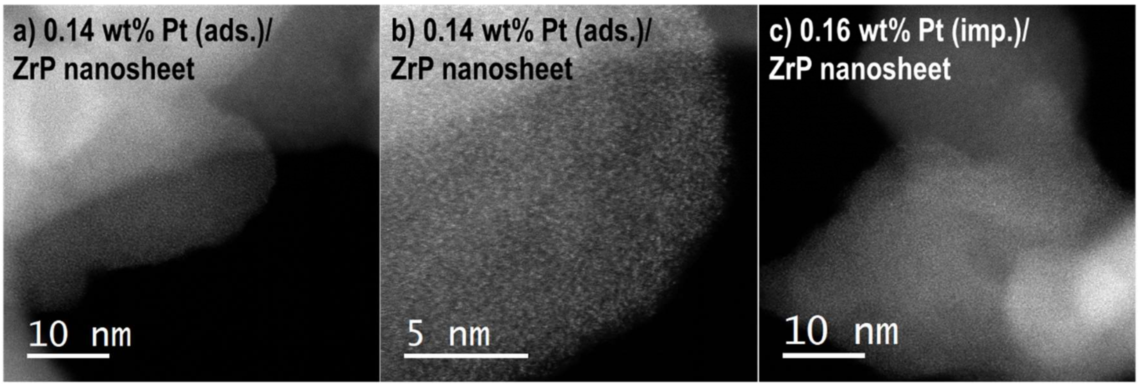

Figure S11. HAADF-STEM images of the (a-b) 0.14 wt% Pt (ads.)/ZrP nanosheet and (c) 0.16 wt% Pt (imp.)/ZrP nanosheet.

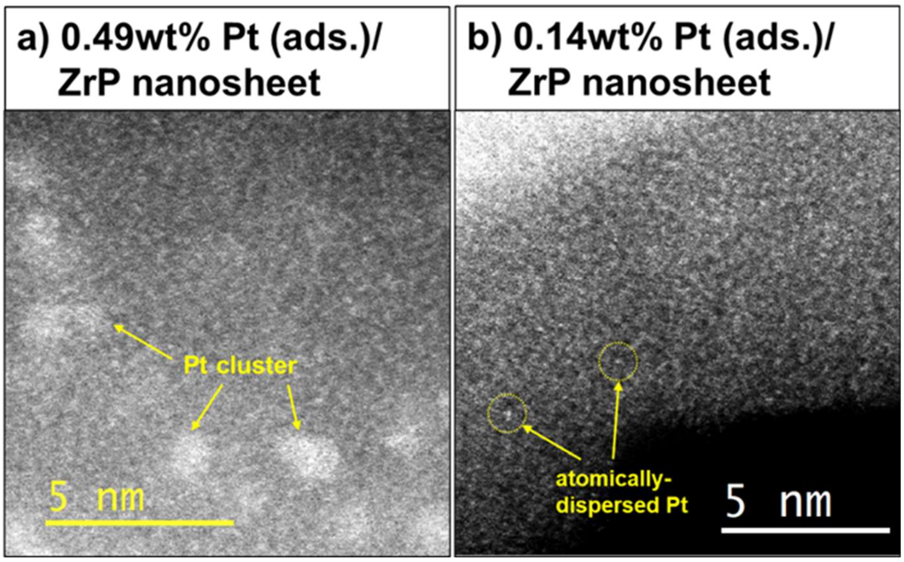

Figure S12. HAADF-STEM images showing Pt clusters and atomically-dispersed Pt on (a) 0.49 wt% Pt (ads.)/ZrP nanosheet and (b) 0.14 wt% Pt (ads.)/ZrP nanosheet.

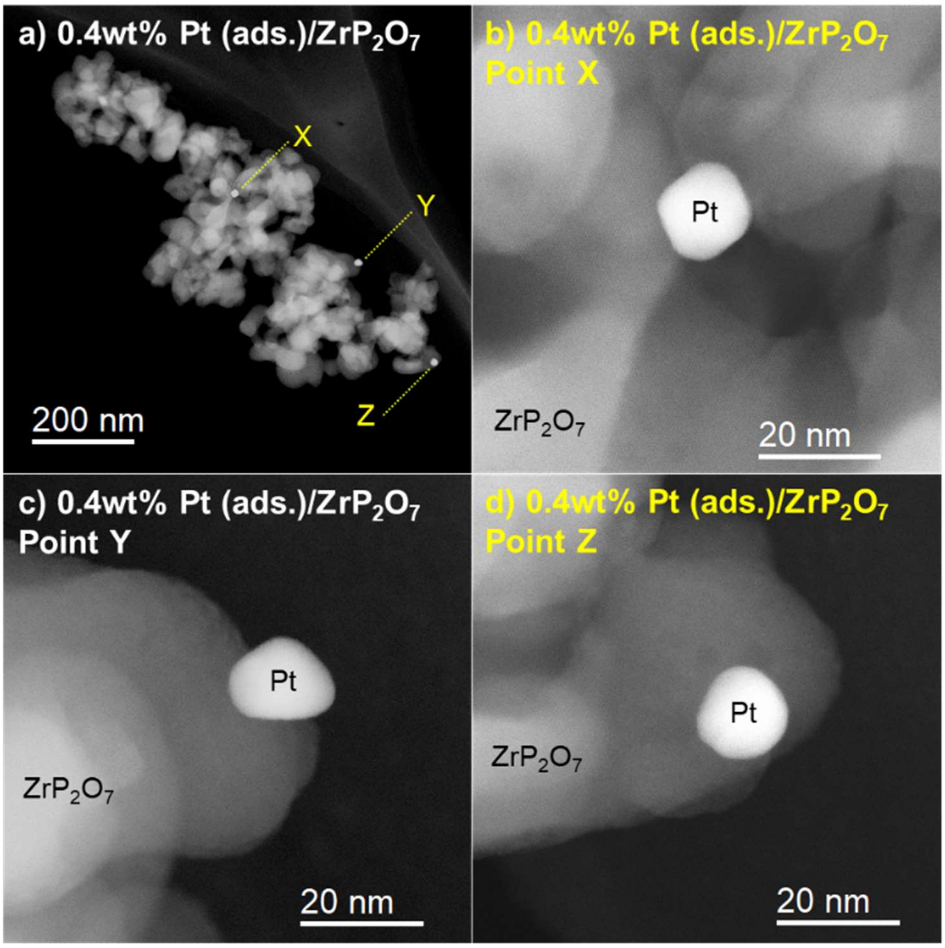

Figure S13. (a-d) HAADF-STEM images of 0.4 wt% Pt (ads.)/ZrP_2O_7. The images (b), (c), and (d) are zoomed images of the area marked by X, Y, and Z in (a).

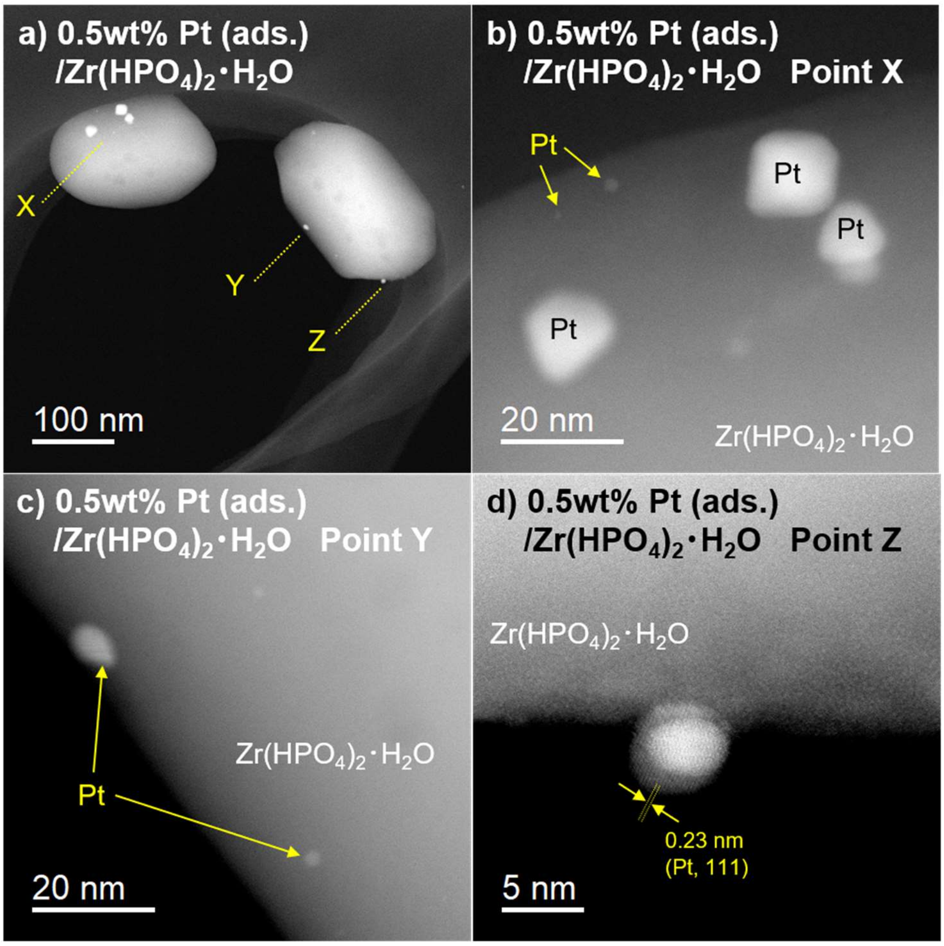

Figure S14. (a-d) HAADF-STEM images of 0.5 wt% Pt (ads.)/α-$Zr(HPO_4)_2 \cdot H_2O$. The images (b), (c), and (d) are zoomed images of the area marked by X, Y, and Z in (a).

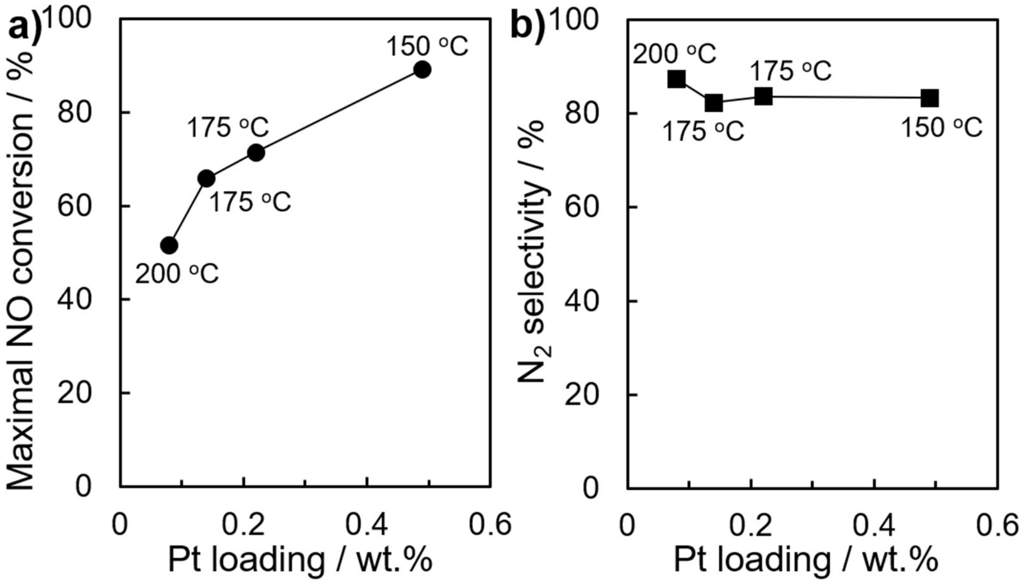

Figure S15. (a) Maximal NO conversion for H_2-SCR over 0.08 (200 °C), 0.14 (175 °C), 0.22 (175 °C), and 0.49 wt% (150 °C) Pt (ads.)/ZrP nanosheet. (b) N_2 selectivity over 0.08-0.49 wt% Pt (ads.)/ZrP nanosheet at the same temperatures for (a).

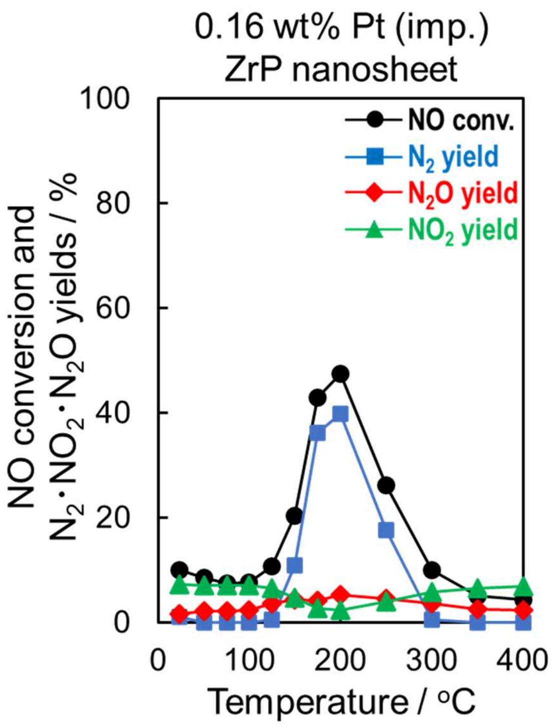

Figure S16. Temperature dependence of NO conversion and product yields over 0.16 wt% Pt (imp.)/ZrP nanosheet. NO (200 ppm), H2 (5,000 ppm), O2 (10%), and He balance.

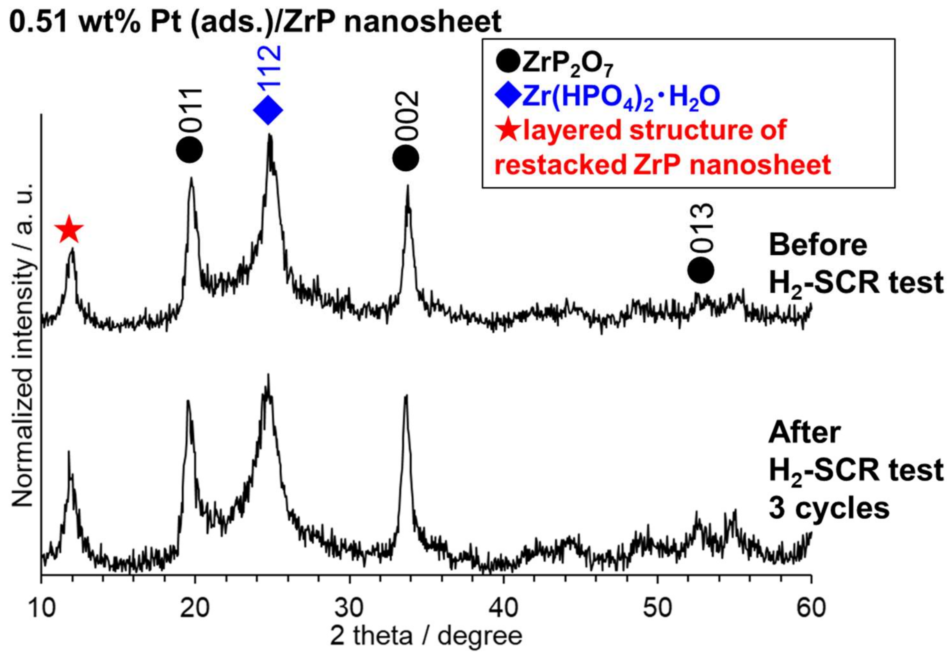

Figure S17. Powder XRD patterns (2θ/θ scan) of the 0.51 wt% Pt (ads.)/ZrP nanosheet before and after examining 3 cycles of H_2-SCR performance test.

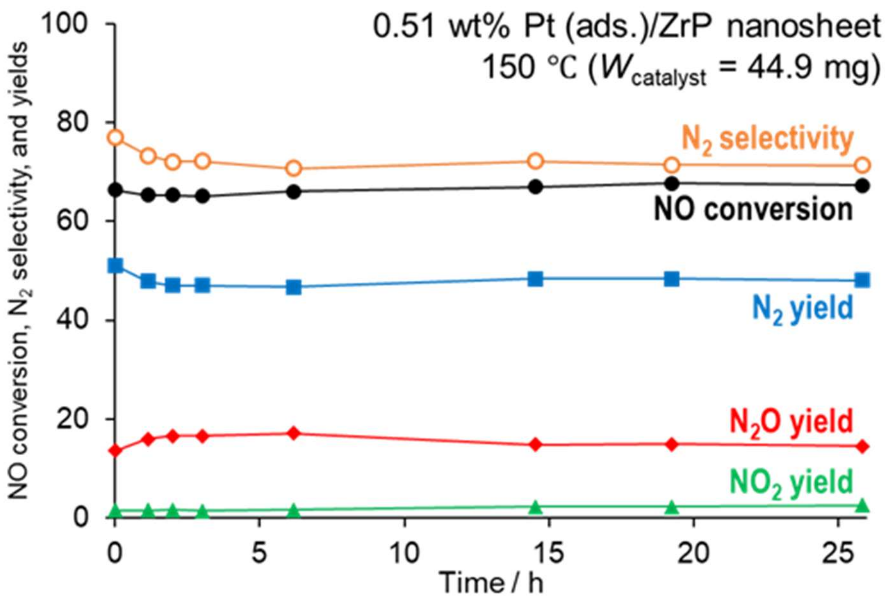

Figure S18. Continuous H_2-SCR performance test over 0.51 wt% Pt (ads.)/ZrP nanosheet at 150 °C in NO (200 ppm), H_2 (5,000 ppm), O_2 (10%), and He balance ($W_{catalyst}$ = 44.9 mg).

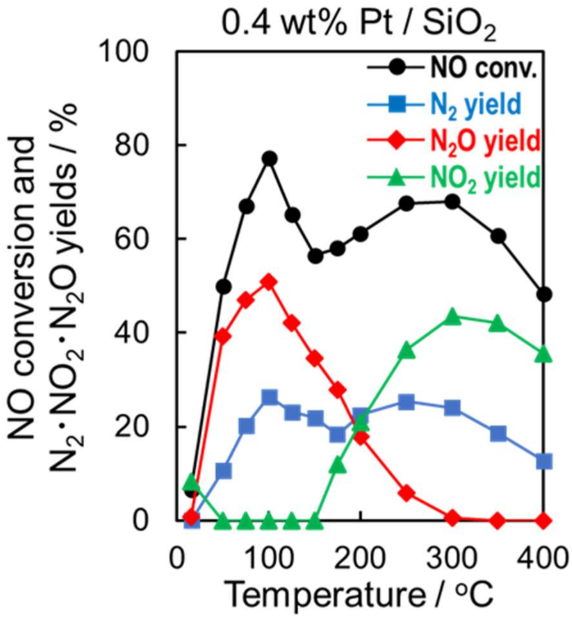

Figure S19. Temperature dependence of NO conversion and product yields over 0.4 wt% Pt/SiO_2. NO (200 ppm), H2 (5,000 ppm), O2 (10%), and He balance.

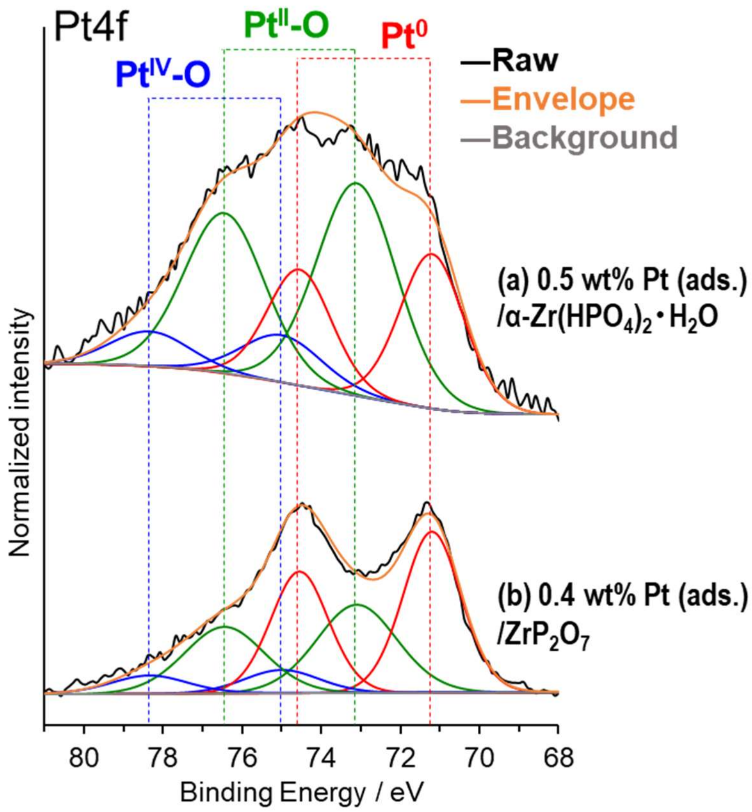

Figure S20. Pt 4f XPS spectra of 0.5 wt% Pt (ads.)/α-$Zr(HPO_4)_2 \cdot H_2O$ and 0.4 wt% Pt (ads.)/ZrP_2O_7. The intensity was normalized using the maximal intensity of Zr3d spectra.

Table S1. BET specific surface area (S_{BET}) of the α-ZrP (α-$Zr(HPO_4)_2 \cdot H_2O$) and its derivatives.

Samples	S_{BET} / m^2/g
α-ZrP (as prepared)	13.2
Restacked ZrP nanosheet (0.1 M HCl)	26.1
Freeze-dried ZrP nanosheet	12.4
HA-intercalated ZrP nanosheet (400 ℃/1 h/air)	40.0
DA-intercalated ZrP nanosheet (400 ℃/1 h/air)	25.3

Table S2. Comparison of the maximal NO_x conversion (conv.), N_2 selectivity, N_2O yield (100 ℃), and NO_2 yield (300 ℃) over the Pt-based H_2-SCR catalyst reported in previous literatures.

Sample	Feed gas composition; Space velocity	Maximal NO_x conv.	N_2 selectivity	N_2O yield at 100 °C	NO_2 yield at 300 °C	Ref.
1wt% Pt/Ti-MCM-41	$NO/H_2/O_2$ = 0.1%/0.5%/6.7%, He balance; 80,000 h^{-1}	88% 140 °C	79% 140 °C	n/a	n/a	[S1]
0.94wt% Pt/Al-MCM-41	$NO/H_2/O_2$ = 0.1%/0.5%/6.7%, He balance; 80,000 h^{-1}	80% 120 °C	85% 120 °C	n/a	n/a	[S2]
1wt% Pt/ZSM-35	$NO/H_2/O_2$ = 0.1%/0.5%/6.7%, He balance; 80,000 h^{-1}	81% 120 °C	69% 120 °C	n/a	n/a	[S3]
0.5wt% Pt/H-FER	$NO/NO_2/H_2/O_2$ = 0.091%/0.009%/0.5%/10%, He balance; 36,000 h^{-1}	87% 110 °C	69% 110 °C	n/a	54%	[S4]
0.5wt% Pt/HY	$NO/H_2/O_2$ = 0.1%/0.5%/10%, He balance; 32,000 h^{-1}	81% 130 °C	75% 130 °C	n/a	n/a	[S5]
1wt% Pt/SSZ-13	$NO/H_2/H_2O/O_2$ = 0.1%/0.5%/5%/10%, He balance; 20,000 h^{-1}	98% 100 °C	23% 100 °C	80%	60%	[S6]
1.5wt% Pt/ZSM-5	$NO/H_2/H_2O/O_2$ = 0.05%/0.5%/5%/5%, He balance; 120,000 ml/h·g_{cat}	99% 75 °C	79% 75 °C	n/a	22%	[S7]
2wt% Pt/MnO_x	$NO/H_2/O_2$ = 0.048%/0.8%/5%, He balance; 78,000 h^{-1}	63% 100 °C	30% 100 °C	34%	n/a	[S8]
1wt% Pt/$Ti_{0.5}Zr_{0.5}$ (TiO_2+ZrO_2+$ZrTiO_4$)	$NO/H_2/O_2$ = 0.03%/0.24%/5%, N_2 balance; 36,000 h^{-1}	97% 130 °C	60% 130 °C	n/a	13% (250 °C)	[S9]
0.49wt% Pt (ads.)/ZrP nanosheet	$NO/H_2/O_2$ = 0.02%/0.5%/10%, He balance; 120,000 ml/h·g_{cat}, ~50,000 h^{-1}	89% 150 °C	83% 150 °C	16%	9%	This work

Table S3. Percentages of Pt species of 0.08-0.49 wt% Pt (ads.)/ZrP nanosheet and 0.16 wt% Pt (imp.)/ZrP nanosheet (XPS analysis).

Pt loading amount of Pt/ZrP nanosheet / wt%	**Method**	**Pt^0 / %**	**Pt^{II}-O / %**	**Pt^{IV}-O / %**
0.08	Ads.	33.4	47.8	18.8
0.14	Ads.	31.4	48.9	19.7
0.22	Ads.	29.3	56.5	14.2
0.49	Ads.	29.2	58.3	12.5
0.16	Imp.	30.4	56.2	13.4

Table S4. Percentages of Pt species of 0.4 wt% Pt (ads.)/ZrP_2O_7 and 0.5 wt% Pt (ads.)/α-$Zr(HPO_4)_2·H_2O$ (XPS analysis).

Samples	**Method**	**Pt^0 / %**	**Pt^{II}-O / %**	**Pt^{IV}-O / %**
0.4 wt% Pt/ZrP_2O_7	Ads.	54.1	32.7	13.2
0.5 wt% Pt/α-$Zr(HPO_4)_2·H_2O$	Ads.	34.4	49.0	16.6

References

[S1] L. Li, P. Wu, Q. Yu, G. Wu, N. Guan, *Appl. Catal. B*, 2010, *94*, 254-262.

[S2] P. Wu, L. Li, Q. Yu, G. Wu, N. Guan, *Catal. Today*, 2010, *158*, 228-234.

[S3] Q. Yu, M. Richter, F. Kong, L. Li, G. Wu, N. Guan, *Catal. Today*, 2010, *158*, 452-458.

[S4] S. Yang, X. Wang, W. Chu, Z. Song, S. Zhao, *Appl. Catal. B*, 2011, *107*, 380-385.

[S5] X. Zhang, X. Wang, X. Zhao, Y. Xu, H. Gao, F. Zhang, *Chem. Eng. J.*, 2014, *252*, 288-297.

[S6] J. Shao, P. H. Ho, D. Creaser, L. Olsson, *Appl. Catal. O*, 2024, *188*, 206947.

[S7] D. C. Park, S. Moon, J. H. Song, H. Kim, E. Lee, Y. H. Lim, D. H. Kim, *Catal. Today*, 2024, *425*, 114318.

[S8] S. M. Park, M. -Y. Kim, E. S. Kim, H. -S. Han, G. Seo, *Appl. Catal. A*, 2011, *395*, 120-128.

[S9] Y. Li, D. He, H. Zhao, M. Pei, Y. Fan, H. Xu, J. Wang, Y. Chen, *Chem. Eng. J.*, 2024, *490*, 151714.